

## Comparison of Iron Accumulation in Clinical MRI Data

<sup>1</sup>M. Masárová, <sup>1</sup>A. Krafčík, <sup>1</sup>M. Teplan, <sup>1</sup>O. Štrbák, <sup>1</sup>D. Gogola, <sup>2</sup>P. Bořuta,  
<sup>1</sup>I. Frollo

<sup>1</sup>Institute of Measurement Science, SAS, Bratislava, Slovakia

<sup>2</sup>Slovak Medical University, Bratislava, Slovakia

Email: marta.masarova@savba.sk

**Abstract.** *The aim of this study is to clarify whether clinical MRI data can be used in evaluation of the pathological processes associated with disrupted iron homeostasis, such as neurodegenerative processes, or cirrhosis. MRI has potential to become a non-invasive biomarker of such pathology, however new quantification methods must be introduced. Our findings confirmed that it is possible to detect significant difference between healthy and pathological tissue from standard T2 weighted MRI protocols. Moreover, diagnostic tool might be developed from our approach, as discriminant analysis yielded 9.7 % overall error rate.*

*Keywords: MRI, Iron, Contrast Change, Neuroinflammation Disease, Human Brain*

### 1. Introduction

Iron is an essential nutrient, required by every human cell. Iron concentration is normally maintained in a narrow homeostatic range, in about 40 mg Fe/kg of body weight in women, and 50 mg Fe/kg in men. [1][2]

The iron in human body has two major forms. Heme and nonheme iron. About 80% of body iron is functional, located in red blood cells as hemoglobin, in muscles as myoglobin, and in muscle, and also as a part of iron-containing enzymes. Nonheme iron can be found in transporter molecules such as transferrin, as well as, in storage molecules such as ferritin and hemosiderin. Transferrin is an intravascular transport protein that delivers iron to the liver, bone marrow, and other tissues. Ferritin is a spherical protein shell, which is able to accumulate and store up to 4500 iron atoms. [1] [3]

Iron plays an important role in the central nervous system (CNS) where it is involved in oxygen transport, neurotransmitter synthesis and nerve myelination [2]. Abnormal accumulation of iron or disruption of iron metabolism has been detected in various liver disease and neurodegenerative diseases such as Parkinson disease (PD) and Sclerosis multiplex (SM). Highest concentrations of iron in neurodegenerative disease were found in basal ganglia and related structures (BGRS): Globus pallidus (21µg/100g fresh weight), Substantia nigra, red nucleus and putamen [1] [2].

Ferritin and hemosiderin are supposed to be the most important sources of iron related to signal changes in cerebral MRI. Presence of iron has influences on the final contrast of T2 weighted MR images. The loss of the signal in T2 weighted images is caused by a shortening of the transversal relaxation times of protons, especially in deep gray matter nuclei of the brain. Such iron caused hypointensive artifacts have a potential to become a new non-invasive tool of iron related disorders. [1]

The aim of this study is to find out, with the help of clinical MRI data, whether it is possible to distinguish between healthy and pathological tissue (with standard MRI protocols), enable such iron quantification and non-invasive diagnostics of iron-related disorders.

## 2. Subject and Methods

The aim of our research is comparison of healthy (control) and pathological clinical MRI data with respect to signal modification caused by biogenic iron accumulation. Clinical data were obtained from the Slovak Medical University Bratislava (ass. prof. P. Boruta), and were measured on 3T system Siemens Vario, by standard T2 weighted GE protocol. 31 persons with different sex and age were evaluated. 18 persons were identified as healthy, and 13 persons were diagnosed as Sclerosis Multiplex (SM) or Parkinson disease (PD) patients. For image data processing and basic analysis we used the following software tools: Marevisi (NRC - Institute for Biodiagnostic, Winipeg, Canada), and Matlab R2011b (Mathworks Inc., Natick, Massachusetts, USA).

The Regions of Interest (ROI), comprising of BGRS as well as reference sites, were identified by radiologist in every evaluated person, for both groups (control and pathological). Relative T2 contrast for every person, every slice, and every ROI was calculated as follows:

$$RC = \frac{(c-c_0)}{c_0} \quad (1)$$

where RC relative contrast,  
 c mean intensity of each sample ROI in MRI image slice,  
 $c_0$  grand mean [4] intensity of all reference ROIs in same MRI image slice.

Standard statistical tools were applied to distinguish between pathology and control sample. Shapiro-Wilk test was used for normal distribution evaluation, and Kruskal-Wallis test to distinguish whether data originate from the same distribution. The control group (healthy subjects) comprises of 281 data samples (ROIs) from 18 subjects, and pathological group (PD or SM patients) includes 138 data samples (ROIs) from 13 subjects.

## 3. Results

Total relative contrast value for control and pathological group is shown in Fig. 1. The result indicates that we are able to clearly distinguish between healthy and diseased group. Statistical tests were applied to verify the significance of such findings. Shapiro-Wilk test has shown that both groups (control, and pathological) were not distributed normally (Fig. 2). Subsequent non-parametric Kruskal-Wallis test confirmed that both groups are very significantly different, with p-value smaller than  $10^{-10}$ .

As the next step we focused on the approach valuable from the diagnostic point of view. Leave-one-out cross-validation was implemented in order to simulate new patient approaching for diagnostics. From 31 subjects each time one subject was omitted, while from the rest of 30 subjects RC distribution for pathological and control groups were separately formed. "New" patient was classified into one of the two groups based on the comparison of his or her distribution of RC with distributions belonging to pathological and control groups. Greater of the two p-values from Kruskal-Wallis test was interpreted in such a way that two distributions under comparison were closer to each other. Thus, the patient was classified just into this group. 11 out of 13 subjects from pathological group were discriminated correctly, which yields 84.6 % sensitivity, or complementarily 15.4 % false negative error rate. For control group, 17 out of 18 subjects were classified correctly, yielding 94.4 % specificity, or 5.6 % false positive error rate. The overall error rate was at the level of 9.7 %. By this procedure we were able to obtain relatively strong discriminating rates in spite of the fact that control and pathological distributions are apparently overlapping to greater extent.

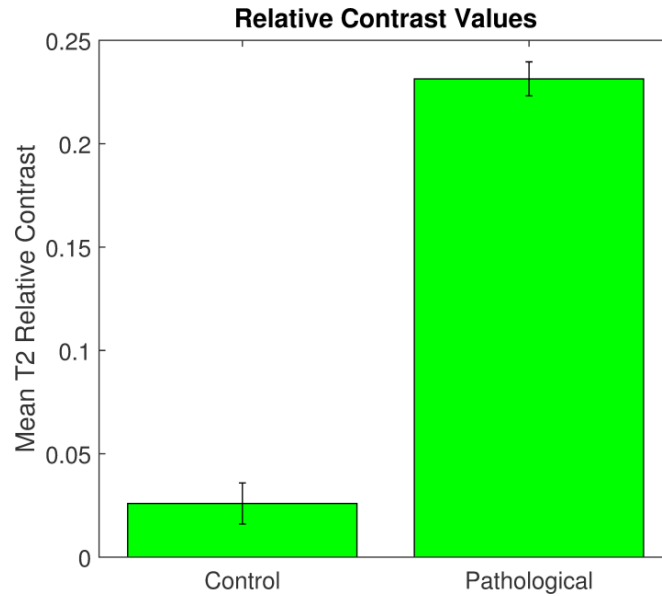


Fig. 1. Relative contrast value for control and pathological group

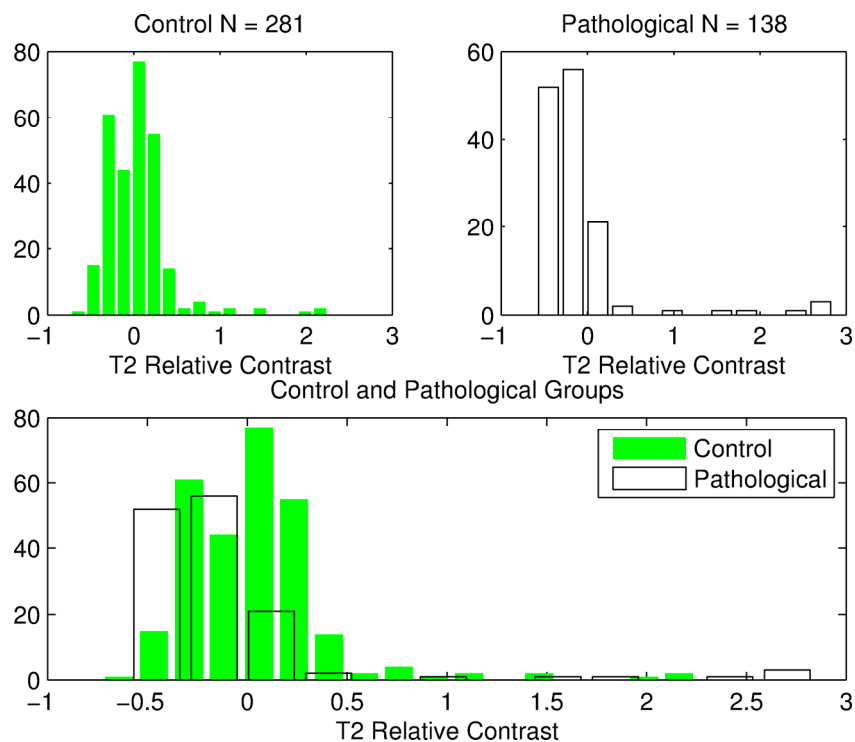


Fig. 2. T2 Relative contrast control and pathological group

#### 4. Conclusions

Statistical evaluation of standard T2 weighted MR images of selected brain tissue objects has shown significant difference between control (without neuropathology) and pathological group, using non-parametric statistical method. Based on these limited data it seems feasible that diagnostic tool for several iron sensitive neurodegenerative conditions may be developed. Outcome of this study is our starting point for further research in the field of iron quantification and non-invasive diagnostics of neuropathological diseases associated with the accumulation of iron in brain tissue.

### **Acknowledgements**

This work was supported by the Slovak Research and Development Agency APVV-0431-12, and by the Slovak Scientific Grant Agency VEGA 2/0013/14, and 2/0043/13.

### **References**

- [1] Dusek P, Dezortova M, Wuerfel J. Imaging of Iron. *International Review of Neurobiology*, 110 (2013), 195-239.
- [2] Sirlin CB, Reeder S B. Magnetic Resonance Imaging Quantification of Liver Iron. *Magn Reson Imaging Clin N Am*, 18 (2010), 359–381.
- [3] You LH, Li F, Wang L, Zhao SE, Wang SM, Zhang LL, Zhang LH, Duan XL, Yu P, Chang YZ. Brain Iron Accumulation Exacerbates the Patogenesis of MPTP-Induced Parkinson`s Disease. *Neuroscience*, 284 (2015), 234-246.
- [4] Burton DA. Composite Standard Deviations. available [online] (March 2015).<[http://www.burtonsys.com/climate/composite\\_standard\\_deviations.html](http://www.burtonsys.com/climate/composite_standard_deviations.html)>.